



OPEN Peripheral blood cellular dynamics during the progression of human tuberculosis

Shanshan Zhu¹✉, Qiuchen Dai^{2,3}, Kai Wang^{2,3}, Hanlin Yan^{2,3}, Yuexuan Ma¹, Yayan Niu⁴, Cheng Chen⁵, Meiyong Wu⁴, Xueying Xie¹ & Wanjun Gu^{2,3,6}✉

Tuberculosis (TB) remains a major global health challenge. Peripheral blood immune cell composition provides valuable insights into TB progression and management. In this study, we analyzed cellular dynamics across the TB disease spectrum using 43 global transcriptomic datasets encompassing 5,902 blood samples. Distinct immune changes were identified during the early stages of TB progression. Transition from latent infection to incipient TB was associated with reduced proportions of natural killer (NK) cells. In subclinical TB, monocyte proportions increased further, accompanied by additional reductions in NK cells and B cells. These early immune shifts preceded the pronounced alterations observed in active TB, characterized by elevated monocytes and neutrophils alongside markedly decreased lymphocyte populations. During successful anti-TB treatment, immune profiles gradually normalized. Cellular dynamics were also influenced by TB burden, age, and HIV coinfection, with stronger immune responses observed in adults and in regions with lower TB burdens. Overall, this study highlights early-stage peripheral blood biomarkers, particularly NK cell changes, as potential indicators of TB progression and targets for preventive interventions.

Keywords Tuberculosis progression, Blood transcriptome, Incipient tuberculosis, Subclinical tuberculosis

Tuberculosis (TB), caused by *Mycobacterium tuberculosis* (*Mtb*), is one of the oldest known diseases and remains the deadliest infectious disease globally¹. In 2023, approximately 10.8 million people were diagnosed with TB, leading to 1.25 million deaths worldwide¹. To combat the ongoing TB epidemic and reduce mortality, the World Health Organization (WHO) set a target in 2015 to “end the TB epidemic by 2035” through proactive screening and preventive treatment for high-risk populations². Early diagnosis and timely intervention are particularly critical for minimizing diagnostic delays and controlling the spread of TB within communities³.

In TB research, examining the cellular composition of peripheral blood can significantly support early diagnosis and intervention across multiple dimensions⁴. First, the immune system’s capacity to recognize and control *Mtb* infection is essential. Peripheral blood is an easily accessible source of immune cells, including monocytes, neutrophils, and T cells. These cells offer valuable insights into the immune responses that influence TB control and progression⁴. For example, CD4⁺ T cells, particularly those that produce interferon gamma (IFN- γ), play a key role in activating macrophages to eliminate bacteria⁵. However, immune response imbalances, such as excessive inflammation or immune suppression, can either improve or worsen TB outcomes⁶. Compared with those with active TB (ATB), people with latent TB infection (LTBI) display a distinct immune cell profile, offering insights into the immune system’s shift from containing bacteria to allowing active disease⁵. Second, the blood immune cell composition can indicate the TB stage and the ability of the body to fight infection. Patients with ATB often exhibit higher levels of proinflammatory cytokines and altered frequencies of monocytes and neutrophils than do those with LTBI or healthy individuals⁷. Additionally, blood tests revealing elevated neutrophil counts or altered monocyte–lymphocyte ratios are commonly linked with severe or disseminated TB⁸. Monitoring these changes enables clinicians to predict disease outcomes and adjust treatment strategies. Third,

¹State Key Laboratory of Bioelectronics, School of Biological Science and Medical Engineering, Southeast University, Nanjing, Jiangsu, China. ²School of Artificial Intelligence and Information Technology, Nanjing University of Chinese Medicine, Nanjing, Jiangsu, China. ³Jiangsu Province Engineering Research Center of TCM Intelligence Health Service, Nanjing University of Chinese Medicine, Nanjing, Jiangsu, China. ⁴Department of Tuberculosis, The Fifth People’s Hospital of Suzhou, The Affiliated Infectious Diseases Hospital of Soochow University, Suzhou, Jiangsu, China. ⁵Department of Chronic Communicable Disease, Center for Disease Control and Prevention of Jiangsu Province, Nanjing, Jiangsu, China. ⁶Collaborative Innovation Center of Jiangsu Province of Cancer Prevention and Treatment of Chinese Medicine, Nanjing University of Chinese Medicine, Nanjing, Jiangsu, China. ✉email: 230198597@seu.edu.cn; wanjungu@njucm.edu.cn

peripheral blood biomarkers are essential for enhancing TB diagnostics and monitoring treatment progress. Cellular markers, such as specific surface protein expression levels (e.g., PD-1 on T cells or CD38 on monocytes) and cytokine production patterns, can indicate TB activity or treatment response. For example, increased CD38⁺ CD4⁺ T cell levels are associated with ATB and can help distinguish ATB from LTBI⁹. Thus, studying peripheral blood cellular compositions is essential for understanding immune responses in TB, assessing disease progression, and identifying diagnostic biomarkers.

The compositional changes in peripheral immune cells during TB development and treatment have been thoroughly explored via blood transcriptomes¹⁰. A pioneering study on blood transcriptomes in ATB patients reported a decrease in lymphocytes, including CD4⁺ T cells, CD8⁺ T cells, and B cells, in ATB patients within the *Leicester* cohort^{11,12}. Furthermore, a reduction in polyfunctional type 17 helper T (Th17) cell-like memory T cells was observed among individuals who progressed from *Mtb* infection to ATB in a *Peruvian* TB progression cohort¹³. In a single-cell transcriptome analysis of peripheral blood samples from healthy controls and LTBI and ATB patients, Cai et al. reported a gradual depletion of CD3⁻ CD7⁺ GZMB⁺ natural killer (NK) cells with TB disease progression in a *Chinese* cohort¹⁴. This depletion of circulating NK cells was reversed following anti-TB treatment (ATT). However, a distinct NK-like CD8⁺ $\gamma\delta$ T cell subset was expanded in patients with persistent *Mtb* infection within the *ACS* cohort¹⁵. Conversely, certain myeloid cells, such as inflammatory monocytes, were found to be elevated in ATB patients^{11,12}. For example, the number of circulating CD14⁺ CD16⁺ monocytes was elevated in ATB patients in one *Chinese* cohort¹⁴. In contrast, Lyu et al. reported no such changes in monocytes in another *Chinese* cohort¹⁶. They only reported a significant decrease in naive CD4⁺ T cells in ATB patients. These findings indicate substantial changes in circulating immune cells across various stages of *Mtb* infection, although the diversity of cellular responses across different cohorts could limit their diagnostic value for TB in practical settings. To strengthen the reliability of these cellular changes as circulating biomarkers during TB development and treatment, Roy Chowdhury et al. performed a computational deconvolution analysis of cell proportions in the peripheral blood across more than 10 clinical cohorts from three continents, including uninfected individuals (UI), LTBI, ATB, and treated TB patients, via blood transcriptomic datasets¹⁷. Their analysis revealed a consistent increase in the number of circulating NK cells in LTBI patients, a decrease in ATB, and a return to baseline following clinical recovery. Importantly, this change in circulating NK cells was further validated in an independent cohort, the *South African* longitudinal cohort, confirming its association with TB progression, treatment response, and the local inflammatory profile in ATB patients¹⁷. This underscores the importance and applicability of integrating heterogeneous datasets to increase the reproducibility, robustness and generalizability of the use of cellular biomarkers for TB diagnosis and treatment^{18,19}.

While existing studies have revealed widespread changes in the circulating blood cell composition during TB development and treatment, most findings rely on a simplified binary classification of TB states—LTBI and ATB. Although this model has helped prevent millions of TB-related deaths, it has had a limited effect on reducing transmission and disease incidence, likely because millions of TB-infected individuals do not seek healthcare or receive treatment²⁰. Recent studies have further refined the classification of asymptomatic LTBI individuals into three categories: LTBI non-progressors (LTBI NP), incipient TB patients (ITB), and subclinical TB patients (STB)^{21,22}. Among these individuals, STB patients contribute significantly to *Mtb* transmission despite showing no clinical symptoms²³. Therefore, a deeper understanding of stage-specific cellular compositional changes throughout the TB spectrum, particularly in the disease's early stages, is essential for advancing knowledge of TB progression and detection²². To meet this need, we expanded our meta-analysis of blood cellular compositions in human TB by including additional public blood transcriptome datasets and categorizing TB-related samples within a framework that considers key asymptomatic stages in the TB disease spectrum²⁰. We conducted a systematic analysis of changes in the circulating blood cell composition following *Mtb* infection and post-TB treatment across global TB cohorts (Fig. 1). Additionally, we examined the impact of potential confounding factors, such as local TB disease burden, age, and HIV coinfection, on these compositional changes throughout TB progression.

Materials and methods

Data collection

We searched for blood transcriptomic datasets related to human TB from NCBI *GEO*²⁴ and EBI *ArrayExpress*²⁵ in April 2024 via the terms “tuberculosis”, “transcriptome”, “*Homo sapiens*”, “whole blood OR peripheral blood mononuclear cells OR PBMCs” (Supplementary Figure S1). This search yielded 43 transcriptomic datasets primarily focused on diagnosing LTBI or ATB, predicting TB progression, or monitoring treatment (Supplementary Table S1; Supplementary Notes, Sect. 1). In total, the dataset comprised gene expression data from 5,902 blood samples across five continents. All raw data were downloaded and processed using a uniform preprocessing procedure to obtain protein-coding gene expression profiles (Supplementary Notes, Sect. 2). We identified that some cohorts included overlapping individuals (Supplementary Table S1). To maximize data availability and completeness, we retained these overlapping samples within their respective cohorts and analyzed each dataset as an independent cohort. These overlaps are unlikely to bias results given the size and diversity of the datasets. Leukocyte proportions were subsequently estimated from gene expression profiles using the *CIBERSORTx*²⁶ cell-mixture deconvolution approach (Supplementary Notes, Sect. 3; Supplementary Figure S2).

Phenotype data processing

For decades, TB disease states have been classified using a binary model of LTBI and ATB²⁷. While widely used, this simple model has several limitations. LTBI individuals are broadly defined as the presence of *Mtb* without clinical TB symptoms or infectiousness, whereas ATB is diagnosed by positive culture or molecular tests accompanied by symptoms such as fever, fatigue, appetite loss, and weight loss. To consolidate evidence on post-infection outcomes, we reviewed definitions of TB disease states from recent studies^{28–30}. These criteria

incorporated immunologic tests (e.g., tuberculin skin test, IFN- γ release assay), microbiologic assessments (e.g., bronchoalveolar lavage, pleural fluid, or sputum culture), radiographic findings (e.g., chest X-ray, PET/CT), and clinical symptoms. Based on these criteria, individuals with recent *Mtb* exposure could be classified into the following groups (Supplementary Figure S4):

1. UI (Uninfected individuals): Individuals uninfected or who cleared bacteria through innate or adaptive immunity during follow-up. Samples with < 6 months of follow-up from the date of blood draw were excluded to minimize misclassification³¹.
2. LTBI NP (Latent TB infection, non-progressors): Infected individuals who remained TB-free during follow-up, with the same exclusion criteria as above³¹.
3. ITB (Incipient TB): Individuals who progress to ATB during follow-up but showed no microbiological evidence, radiological abnormalities, or clinical symptoms at the time of blood draw.
4. STB (Subclinical TB): Individuals who progress to ATB during follow-up, showing no clinical symptoms but presenting with immunological, microbiological, or radiological abnormalities at the time of blood draw. Cases with subsequent remission were excluded to reduce misclassification.
5. ATB (Active TB): Newly diagnosed cases or cases detected through passive surveillance, defined by the presence of clinical symptoms, radiological abnormalities, and microbiological evidence.

To analyze cellular changes across TB stages, particularly the early asymptomatic stages, we redefined TB disease states in 37 cross-sectional studies based on these criteria. We also standardized the timing of blood samples for contacts who developed ATB as “time to diagnosis” across 43 datasets, enabling sequential assessment of TB progression (Supplementary Notes, Sect. 4). Healthy controls were annotated as UIs for consistency (Supplementary Table S1). Additionally, samples were grouped by TB burden, age, and HIV status to assess the influence of potential confounding factors (Supplementary Notes, Sect. 4).

Blood cellular composition comparison

To enhance robustness, we conducted multi-cohort case-control comparisons of blood cellular composition across different TB stages in both cross-sectional and longitudinal cohorts. A bivariate meta-analysis (sample size ≥ 5) with a random-effects model¹⁷ was performed using *MetaIntegrator*³². The resulting summary effect size (*ES*) indicated whether cellular proportions increased or decreased across disease stages (Supplementary Notes, Sect. 5.1). To assess the heterogeneity of *ES* estimates across studies, we also calculated a consistency score (*C_score*). To account for potential confounding factors such as country, age, and HIV coinfection, comparisons were further adjusted using linear regression (Supplementary Notes, Sect. 5.2). Group-wise analyses were then performed to evaluate compositional differences by age group, TB burden, and HIV status, with summary *ES* values from the meta-analysis serving as the comparison metric (Supplementary Notes, Sect. 5.3). Statistical significance was assessed using a false discovery rate (*FDR*) threshold of 0.1.

Results

Changes in peripheral blood cell composition in LTBI and ATB

We estimated the proportions of two myeloid cell types (monocytes and neutrophils) and four lymphocyte types (CD8⁺ T cells, CD4⁺ T cells, NK cells, and B cells) from 5,902 blood samples across all transcriptomic datasets (Supplementary Table S1; Supplementary Figure S3). Using these estimates, we first categorized TB-related samples according to the classical binary model and compared the cellular compositions of LTBI individuals and ATB patients with those of UI individuals (Fig. 1A).

In LTBI individuals, monocyte exhibited the most significant increase ($ES=0.345$, $FDR<0.001$), with largely consistent results ($C_score=0.429$) across 14 cohorts (Fig. 2A and B; Supplementary Tables S3A, S4A). No significant changes were observed in the proportions of neutrophils, CD4⁺ T cells, CD8⁺ T cells, NK cells, or B cells (Supplementary Figure S5A; Supplementary Table S4A). In ATB patients, cellular shifts were more pronounced across 20 global cohorts (Fig. 2A and C; Supplementary Figure S5B; Supplementary Tables S3B, S4B). Monocyte ($ES=1.502$, $FDR<0.001$) and neutrophil proportions ($ES=0.386$, $FDR<0.001$) significantly increased, while CD4⁺ T cells ($ES = -0.76$, $FDR<0.001$), CD8⁺ T cells ($ES = -0.516$, $FDR<0.001$), NK cells ($ES = -0.751$, $FDR<0.001$), and B cells ($ES = -0.507$, $FDR<0.001$) significantly decreased. These compositional changes, particularly the monocyte increase, were consistent across cohorts ($C_score=0.9$). Notably, these changes remained robust after adjustment for country, age, and HIV status (Supplementary Figures S6A, S6B; Supplementary Table S5A). A direct comparison of LTBI and ATB individuals across 25 cohorts revealed patterns similar to those observed between ATB and UI individuals (Fig. 2A; Supplementary Figure S5C; Supplementary Tables S3C, S4C).

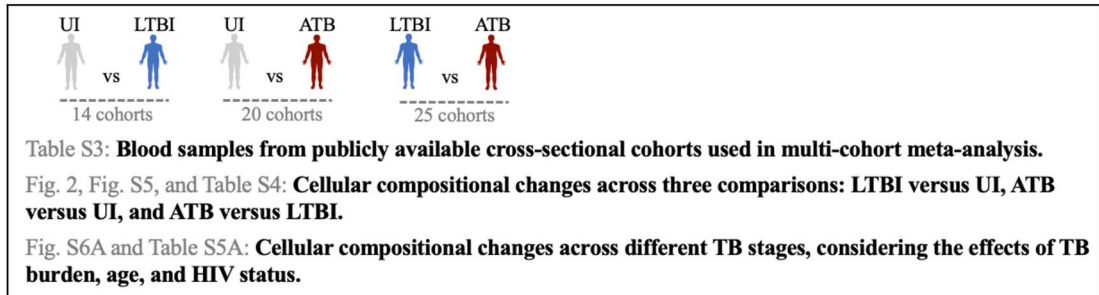
Overall, these findings indicate that immune compositional changes begin in the LTBI state, characterized by monocyte expansion, are broadened to involve all major blood cell types as the disease progresses to ATB.

Changes in peripheral blood cell composition during the early stages of TB development

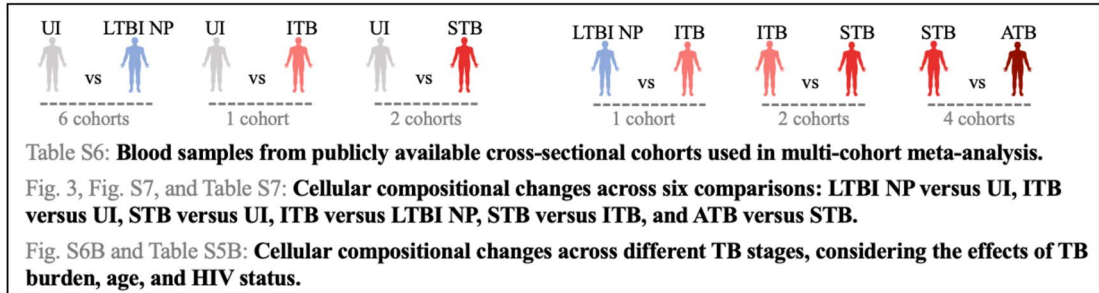
In the previous multi-cohort analysis, LTBI individuals were defined as those infected with *Mtb* but without progression to disease. Under this framework, early-stage cellular changes remain poorly understood, despite some compositional alterations observed in LTBI individuals. To address this gap, we examined cellular shifts more closely, as they may provide insights for preventive therapies and reduce *Mtb* transmission (Fig. 1B).

In the revised TB disease spectrum framework, asymptomatic LTBI individuals were further classified into three groups: LTBI NP, ITB, and STB. We compared blood cell proportions in these asymptomatic states with those in UI individuals across multiple global cohorts. Among LTBI NP individuals, no significant differences in myeloid or lymphocyte cell compositions were observed compared with UI individuals across six cohorts

A. Compositional changes of blood cells in LTBI individuals and ATB patients across global cohorts



B. Compositional changes of blood cells in the early stages of TB development across global cohorts



C. Temporal changes in peripheral blood cell compositions during TB progression

Table S8: Blood samples from publicly available longitudinal cohorts used in multi-cohort meta-analysis. Fig. 4A, Fig. S8, and Table S9: Cellular compositional changes in contacts from 5 cohorts who progressed to ATB over time during TB progression. Fig. 4E and Fig. S9: TB progressors in the *Zak_SA* cohort sampled at different time points before diagnosis. Fig. 4F and Fig. S10: TB progressors in the *Suliman_GC6-74* cohort sampled at different time points before diagnosis. Fig. S11-S12: TB progressors in the *Singhania_Leicester* and *Tabone_Leicester* cohorts sampled at different time points before diagnosis.

D. Temporal changes in peripheral blood cell compositions during TB treatment

Table S10: Blood samples from publicly available longitudinal cohorts used in multi-cohort meta-analysis with or without treatment outcomes. Fig. 5A, Fig. 5B, Fig. S13, and Table S11: Cellular compositional changes in patients with ATB from 9 cohorts over time after TB treatment. Fig. 5C, Fig. S15, and Table S12A-C: Cellular compositional changes in the *Tompson_SA* cohort for monitoring TB treatment. Fig. 5D, Fig. S14, Fig. S16, and Table S12D-H: Cellular compositional changes in the *Tabone_Leicester* cohort for monitoring TB treatment.

E. Effect of confounding factors on blood cellular changes during TB development

Fig. 6A, Fig. S17A, and Table S13: Comparison of cohort-summary effect sizes between TB high- and low-burden countries. Fig. 6B, Fig. S17B, and Table S14: Comparison of cohort-summary effect sizes between different age groups. Fig. S17C and Table S15: Comparison of cohort-summary effect sizes in individuals without HIV co-infection.

(Fig. 3A; Supplementary Figure S7A; Supplementary Tables S6A, S7A). In ITB patients, NK cells were significantly decreased in one cohort ($ES = -1.249$, $FDR = 0.005$; Fig. 3A; Supplementary Figure S7B; Supplementary Tables S6B, S7B). Among STB patients, monocyte proportions significantly increased across two cohorts ($ES = 1.121$, $FDR < 0.013$; Fig. 3A and B; Supplementary Tables S6C, S7C), whereas NK cells ($ES = -0.605$, $FDR = 0.055$) and B cells ($ES = -0.839$, $FDR = 0.004$) significantly decreased. Neutrophils tended to increase and T cells to decrease across cohorts, although these changes did not reach statistical significance (Fig. 3A and B; Supplementary Figure S7C). Importantly, these compositional shifts remained after adjusting for country, age, and HIV status,

Fig. 1. Schematic framework of the experimental design. **(A)** Multi-cohort analysis of changes in circulating blood cell compositions during the latent TB infection (LTBI) and active disease (ATB) stages. **(B)** The latent infection stage was further subdivided into three asymptomatic stages: latent infection without disease progression (LTBI NP), incipient TB (ITB), and subclinical TB (STB). Compositional changes during the early stages of TB development were analyzed through multi-cohort comparisons. **(C)** Temporal changes in circulating blood cell compositions were examined in longitudinal cohorts of individuals who eventually progressed to ATB. **(D)** Temporal variations in blood cell proportions were analyzed in TB patients receiving anti-tuberculosis treatment (ATT). **(E)** The effects of factors such as TB burden, age, and HIV coinfection on cellular changes in circulating blood during TB development were also investigated.

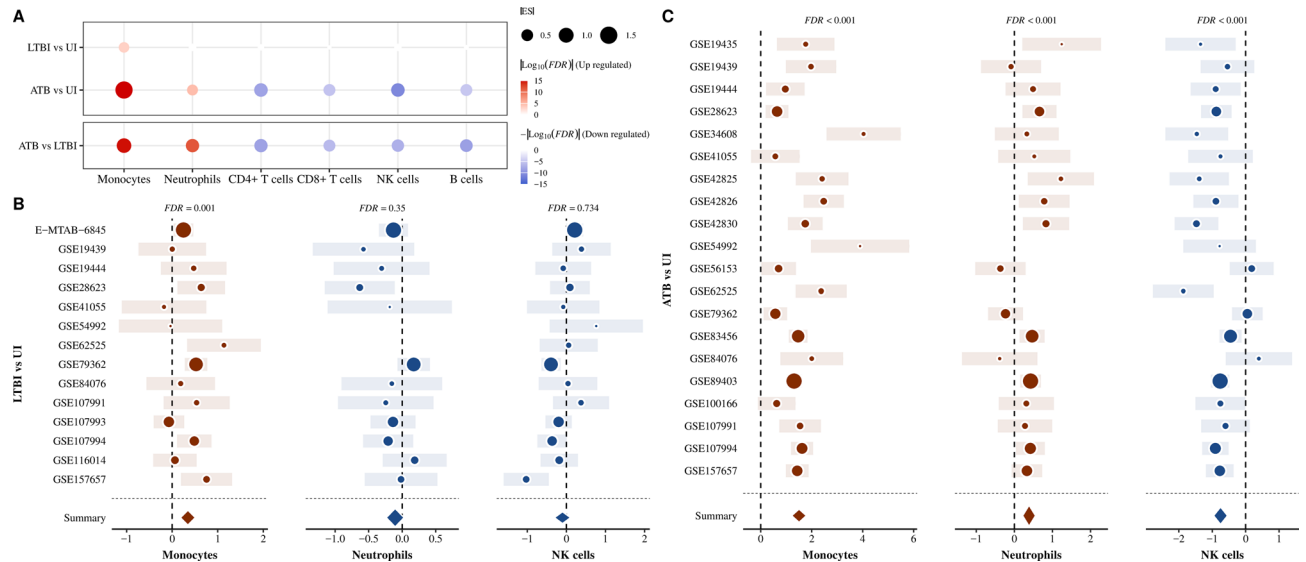


Fig. 2. Compositional changes in peripheral blood cells among LTBI individuals and ATB patients across global cohorts. **(A)** Bubble plot illustrating the compositional changes in six cell types across three comparisons: LTBI individuals versus UI patients, ATB patients versus UI patients, and ATB patients versus LTBI individuals. Red bubbles indicate an increase in the cellular composition, whereas blue bubbles indicate a decrease. The intensity of the color reflects the degree of change, with a false discovery rate (*FDR*) threshold of 0.1 for statistical significance. The bubble size represents the absolute magnitude of the effect size. White circles denote comparisons with no significant differences. **(B)** Forest plots showing the compositional changes in monocytes, neutrophils, and NK cells between LTBI individuals and UI patients. **(C)** Forest plots depicting the compositional changes in monocytes, neutrophils, and NK cells between ATB patients and UI patients. The *GEO* or *ArrayExpress* identifiers represent individual cohorts. Each circle indicates the standardized mean difference (effect size, *ES*) in cellular composition between two groups, with the circle size proportional to the cohort sample size. The horizontal strip of each circle denotes the 95% confidence interval for the *ES*. The diamond represents the overall difference in cellular proportions between two groups, derived by integrating *ES* values from all cohorts (Summary). The *FDR* value indicates the statistical significance of the overall cellular compositional difference across cohorts.

suggesting they were driven primarily by disease progression (Supplementary Figures S6C, S6D; Supplementary Table S5B).

We next examined changes between consecutive disease stages (Fig. 1B). No significant differences were found between LTBI NP and ITB, or between ITB and STB (Fig. 3A; Supplementary Figures S7D, S7E; Supplementary Tables S6D, S6E, S7D, S7E). By contrast, prominent changes were observed between STB and ATB patients across four cohorts (Fig. 3A; Supplementary Tables S6F, S7F). Among myeloid cells, monocytes showed significant increases in ATB patients ($ES = 0.664$, $FDR = 0.027$), whereas neutrophils displayed a non-significant upward trend ($ES = 0.508$, $FDR = 0.237$; Fig. 3C). Among lymphocytes, $CD4^+$ T cells were significantly reduced in ATB ($ES = -0.692$, $FDR = 0.001$), while $CD8^+$ T cells ($ES = -0.381$, $FDR = 0.199$), NK cells ($ES = -0.415$, $FDR = 0.191$), and B cells ($ES = -0.382$, $FDR = 0.237$) all demonstrated downward but non-significant trends (Supplementary Figure S7F).

In summary, no significant compositional changes were detected in the non-infectious stage of TB across these limited cohorts. NK cell reduction emerged early during progression to ITB, followed by increased monocytes and decreased B cells in STB. The transition from STB to ATB was marked by further monocyte expansion alongside significant $CD4^+$ T cell depletion.

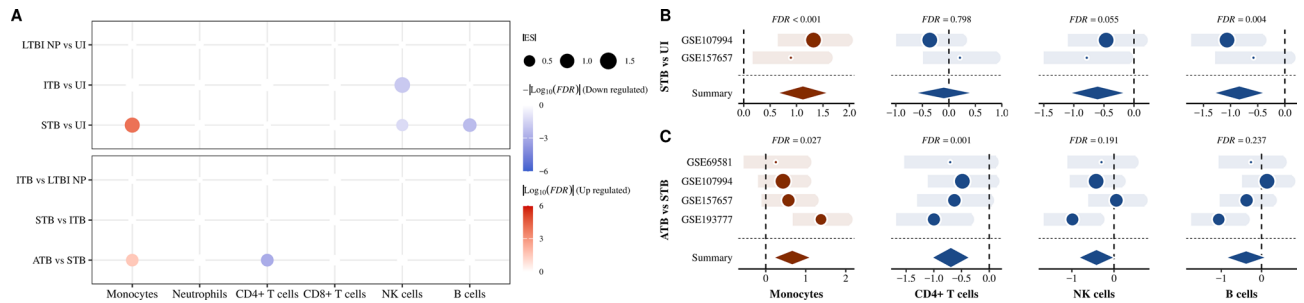


Fig. 3. Compositional changes in peripheral blood cells during the early stages of TB development across global cohorts. **(A)** Bubble plot illustrating compositional changes in six cell types across various comparisons: LTBI NP versus UI individuals, ITB patients versus UI individuals, STB patients versus UI individuals, ITB patients versus LTBI NP individuals, STB patients versus ITB patients, and ATB patients versus STB patients. Red bubbles indicate an increase in the cellular composition, whereas blue bubbles indicate a decrease. The intensity of the color reflects the degree of change, with a false discovery rate (*FDR*) threshold of 0.1 for statistical significance. The bubble size represents the absolute magnitude of the effect size. White circles denote comparisons with no significant differences. **(B)** Forest plots showing compositional changes in monocytes, CD4⁺ T cells, NK cells, and B cells between STB patients and UI patients. **(C)** Forest plots showing compositional changes in monocytes, CD4⁺ T cells, NK cells, and B cells between ATB and STB patients. The *GEO* or *ArrayExpress* identifiers represent individual cohorts. Each circle indicates the standardized mean difference (effect size, *ES*) in cellular composition between two groups, with the circle size proportional to the cohort sample size. The horizontal strip of each circle denotes the 95% confidence interval for the *ES*. The diamond represents the overall difference in cellular proportions between two groups, derived by integrating *ES* values from all cohorts (Summary). The *FDR* value indicates the statistical significance of the overall cellular compositional difference across cohorts.

Temporal changes in peripheral blood cell composition during TB progression

Several longitudinal studies have investigated temporal changes in peripheral blood transcriptomes as TB contacts progress from TB infection to ATB^{28,33–36}. These studies provide valuable insights into the cellular dynamics preceding clinical diagnosis, using cohorts such as *Zak_SA*³³, *Suliman_GC6-74*³⁴, *Singhania_Leicester*³⁵, *Tabone_Leicester*²⁸, and *Roe_UK*³⁶ cohorts (Fig. 1C; Supplementary Table S8). We divided longitudinal blood samples into six time periods (Supplementary Notes, Sect. 4) preceding TB diagnosis and compared cell compositions at each interval to those of UI individuals.

Monocyte proportions began increasing as early as 360–540 days before diagnosis ($ES = 0.649$, $FDR = 0.002$) and continued to rise at 360–180 days before diagnosis ($ES = 1.066$, $FDR = 0.016$; Fig. 4A and B). Between 180 and 60 days prior to diagnosis, significant reductions in B cells were observed ($ES = -0.463$, $FDR = 0.022$; Fig. 4A and C; Supplementary Figure S8C). Interestingly, compositional changes became less pronounced as diagnosis approached, in contrast to patterns observed in cross-sectional cohorts (Figs. 4A; Supplementary Figure S8; Supplementary Tables S9). Monocytes nevertheless exhibited a consistent increase between 60 and 21 days before diagnosis ($ES = 1.245$, $FDR < 0.001$; $C_score = 1$; Fig. 4A; Supplementary Figure S8E). In the final 21 days before diagnosis, monocytes ($ES = 1.222$, $FDR < 0.001$), NK cells ($ES = -0.978$, $FDR < 0.001$), and B cells ($ES = -0.82$, $FDR < 0.001$; Fig. 4A and D; Supplementary Figure S8F) all underwent significant compositional changes. These results demonstrate that peripheral blood cell alterations occur in distinct temporal patterns throughout TB progression.

We further examined the compositional changes in individual TB progressors across four longitudinal cohorts: *Zak_SA*³³, *Suliman_GC6-74*³⁴, *Singhania_Leicester*³⁵, and *Tabone_Leicester*²⁸ cohorts (Fig. 1C). In the *Zak_SA* cohort, nine out of eighteen progressors exhibited the highest proportion of monocytes in the earliest time period before diagnosis (Fig. 4E). Some individuals, such as patients 06_0127 and 07_0259, showed a decrease in monocyte proportions as disease advanced. In the *Suliman_GC6-74* cohort, seven of twenty progressors displayed rising monocyte proportions during follow-up (Fig. 4F). Similar but heterogeneous patterns were observed in the *Singhania_Leicester* (Supplementary Figure S9) and *Tabone_Leicester* (Supplementary Figure S10) cohorts, where only ~50% of progressors demonstrated monocyte increase prior to diagnosis. For NK cells, reductions were detected in eight of eighteen progressors in the *Zak_SA* cohort (Fig. 4E) and eight of twenty in the *Suliman_GC6-74* cohort (Fig. 4F). In contrast, more than two-thirds of progressors in the *Singhania_Leicester* and *Tabone_Leicester* cohorts exhibited NK cell declines (Supplementary Figures S9, S10). Considerable heterogeneity was also evident in other blood cell types, including B cells, T cells, and neutrophils (Supplementary Figures S9–S12).

Collectively, these findings reinforce the overarching trend of monocyte expansion and concomitant NK and B cell decline during TB progression. However, substantial inter-patient and inter-cohort variability in blood cell dynamics was observed. While monocyte increases were consistent across all time periods, other blood cell populations showed fluctuating changes at different intervals. The earliest detectable alterations occurred between 360 and 60 days prior to TB diagnosis, marking a critical window in TB development.

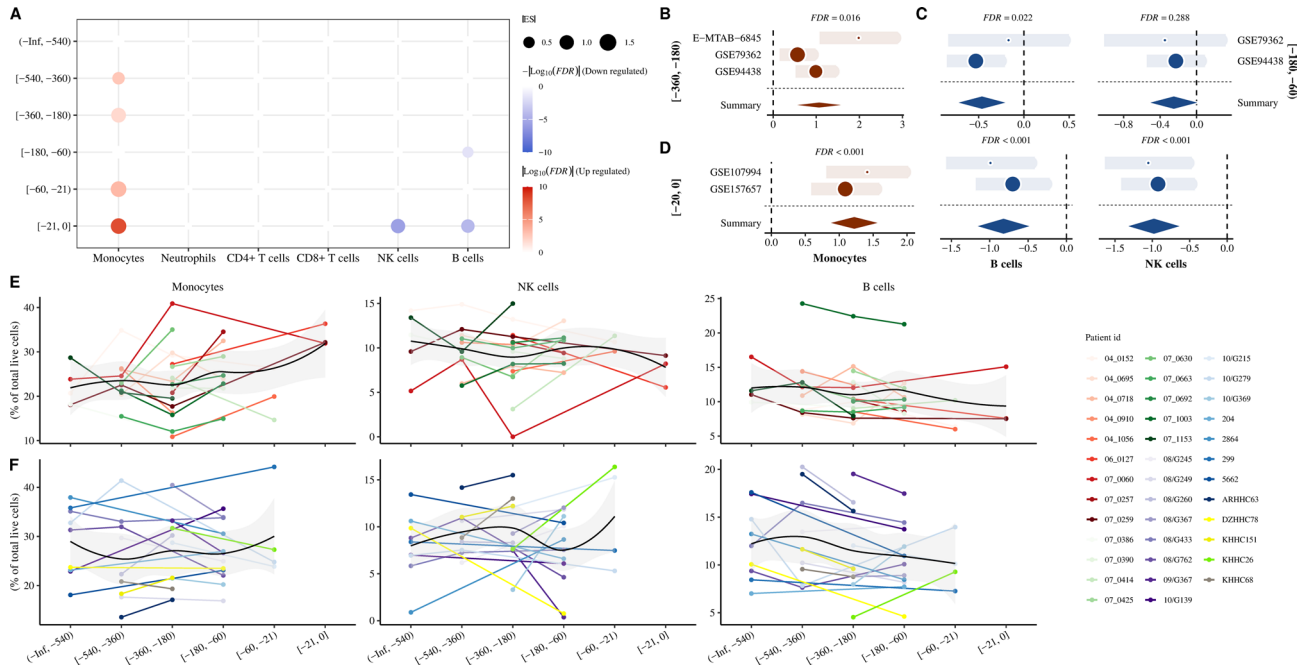


Fig. 4. Temporal changes in peripheral blood cell compositions during TB progression across global cohorts. **(A)** Bubble plot illustrating the compositional changes in six cell types among TB contacts at six intervals relative to TB diagnosis: (-inf, -540), [-540, -360), [-360, -180), [-180, -60), [-60, -21), and [-21, 0] days. Red bubbles indicate an increase in the cellular composition, whereas blue bubbles indicate a decrease. The intensity of the color reflects the degree of change, with a false discovery rate (*FDR*) threshold of 0.1 for statistical significance. The bubble size represents the absolute magnitude of the effect size. White circles denote comparisons with no significant differences. Forest plots highlight specific compositional changes: **(B)** monocytes in TBs contact between 360 and 180 days before diagnosis; **(C)** B cells and NK cells in TBs contact between 180 and 60 days before diagnosis; **(D)** monocytes, B cells, and NK cells in TBs contact 21 days before diagnosis. The *GEO* or *ArrayExpress* identifiers represent individual cohorts. Each circle indicates the standardized mean difference (effect size, *ES*) in cellular composition between two groups, with the circle size proportional to the cohort sample size. The horizontal strip of each circle denotes the 95% confidence interval for the *ES*. The diamond represents the overall difference in cellular proportions between two groups, derived by integrating *ES* values from all cohorts (Summary). The *FDR* value indicates the statistical significance of the overall cellular compositional difference across cohorts. Temporal compositions of monocytes, NK cells, and B cells in individual ATB progressors across six intervals before diagnosis in the **(E)** *Zak_SA* and **(F)** *Suliman_GC6-74* cohorts. The gray shaded area represents the 95% confidence interval for the mean cellular compositions in ATB progressors.

Temporal changes in peripheral blood cell composition during ATT

In addition to pre-diagnosis changes, longitudinal cohorts have also provided insights into how peripheral blood cell compositional shifts during ATT. Using data from nine global cohorts, we tracked cellular dynamics across four intervals following treatment initiation: [7, 28], (28, 60], (60, 182], and (182, 360] days during ATT (Fig. 1D; Supplementary Table S10A). Compared with untreated ATB patients, myeloid cell populations (monocytes and neutrophils) progressively declined, while lymphocyte populations (CD4⁺ T cells, CD8⁺ T cells, NK cells, and B cells) increased (Fig. 5A; Supplementary Table S11; Supplementary Figure S13).

During the early treatment phase (7–28 days post-treatment), monocytes decreased significantly (*ES* = -0.702, *FDR* < 0.001; Fig. 5A and B), accompanied by increases in CD4⁺ T cells (*ES* = 0.32, *FDR* = 0.053), CD8⁺ T cells (*ES* = 0.494, *FDR* = 0.004), and NK cells (*ES* = 0.383, *FDR* = 0.019). Neutrophil reductions emerged between 28 and 60 days (*ES* = -0.538, *FDR* = 0.018), and B cell expansion became evident between 60 and 182 days (Fig. 5A and C). By 60–182 days and extending to 360 days post-treatment, significant shifts were observed across all major cell types, coinciding with the presumed clinical cure of ATB patients (Supplementary Figure S13).

To explore the relationship between these compositional changes and treatment outcomes, we analyzed the *Thompson_SA* cohort³⁷, where patients were categorized as “cured”, “probable cured”, or “not cured” (Supplementary Table S10B). Cured patients exhibited rapid reductions in monocytes and increases in CD4⁺ and CD8⁺ T cells within the first 7 days, followed by declined neutrophils during days 14–30 days (Fig. 5D; Supplementary Table S12A). These patterns mirrored the global cohort trends. In contrast, the “probable cured” group showed more gradual changes (Supplementary Table S12B), while the “not cured” group exhibited minimal alterations – most notably, no significant changes in monocytes or B cells and only a modest NK cell increase between 120 and 180 days (Supplementary Table S12C). A similar pattern was observed in the *Tabone_Leicester*²⁸ cohort (Supplementary Table S10B). Patients requiring extended ATT resembled the “probable cured”

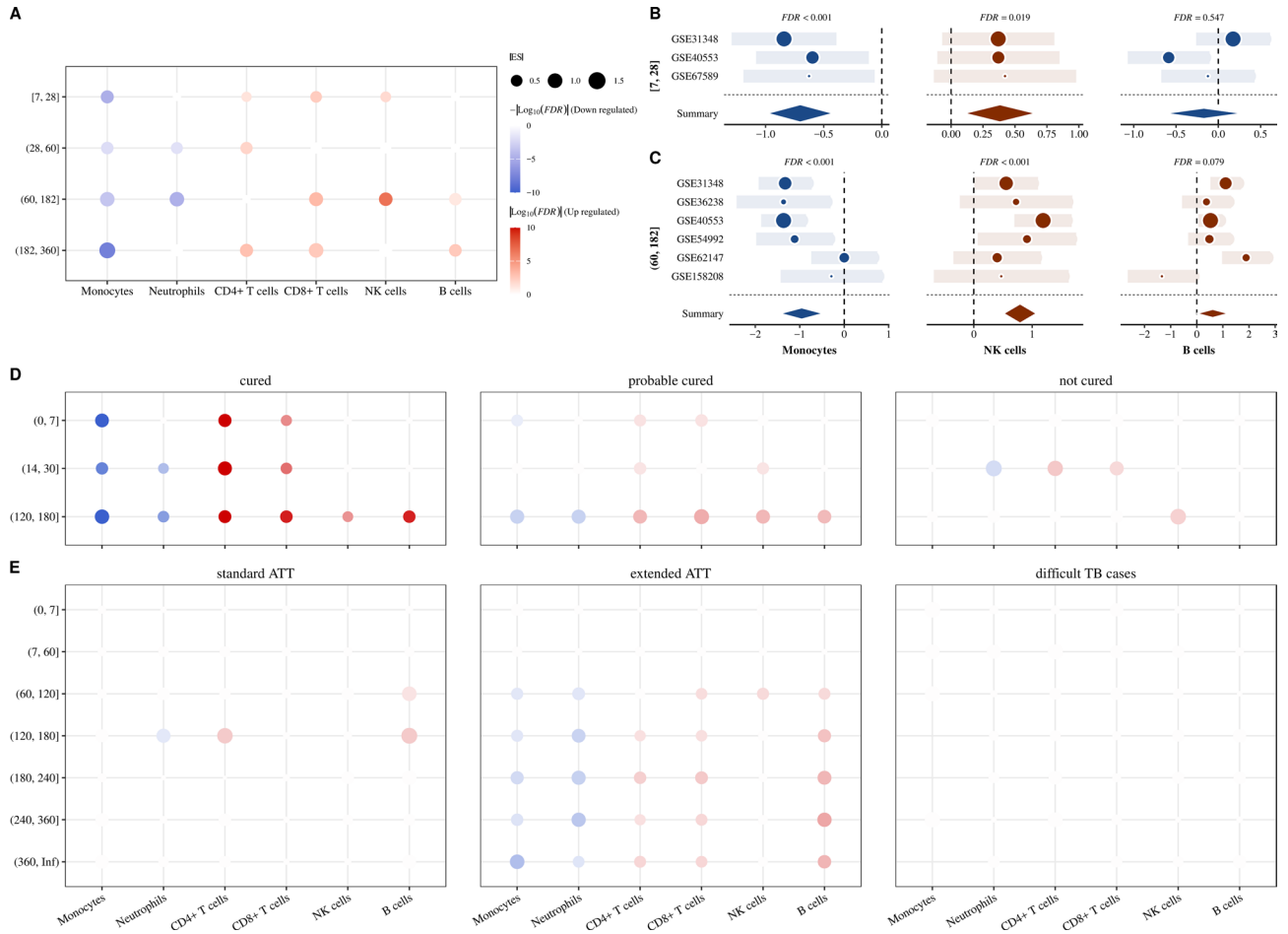


Fig. 5. Temporal changes in peripheral blood cell compositions during ATT across global cohorts. **(A)** Bubble plot showing compositional changes in six cell types in ATB patients across four intervals relative to ATT: [7, 28], (28, 60], (60, 182], and (182, 360] days. Red bubbles indicate an increase in the cellular composition, whereas blue bubbles indicate a decrease. The intensity of the color reflects the degree of change, with a false discovery rate (*FDR*) threshold of 0.1 for statistical significance. The bubble size represents the absolute magnitude of the effect size. White circles denote comparisons with no significant differences. Forest plots illustrate specific compositional changes in monocytes, NK cells, and B cells **(B)** between 7 and 28 days after ATT and **(C)** between 60 and 182 days after ATT. The *GEO* or *ArrayExpress* identifiers represent individual cohorts. Each circle indicates the standardized mean difference (effect size, *ES*) in cellular composition between two groups, with the circle size proportional to the cohort sample size. The horizontal strip of each circle denotes the 95% confidence interval for the *ES*. The diamond represents the overall difference in cellular proportions between two groups, derived by integrating *ES* values from all cohorts (Summary). The *FDR* value indicates the statistical significance of the overall cellular compositional difference across cohorts. **(D)** Bubble plot showing changes in six cell types across three intervals relative to ATT: (0, 7], (14, 30], and (120, 180] days in the *Thompson_SA* cohort. ATB patients in this cohort were grouped by treatment outcome into cured, probable cured, and not cured subgroups. **(E)** Bubble plot showing changes in six cell types across seven intervals relative to ATT: (0, 7], (7, 60], (60, 120], (120, 180], (180, 240], (240, 360], and (360, inf) days in the *Tabone_Leicester* cohort. ATB patients in this cohort were categorized into five subgroups on the basis of clinical information related to ATT: standard ATT, extended ATT, difficult TB cases, TB drug-resistant, and outbreak TB strain subgroups. Bubble plots of the first three subgroups (standard ATT, extended ATT, and difficult TB cases) are shown. Red bubbles indicate an increase in the cellular composition, whereas blue bubbles indicate a decrease. The intensity of the color reflects the degree of change, with a *FDR* threshold of 0.1 for statistical significance. The bubble size represents the absolute magnitude of the effect size. White circles denote comparisons with no significant differences.

group, with significant shifts in most cell types occurring only after 60 days (Fig. 5D and E; Supplementary Table S12E). By contrast, patients on standard ATT displayed much weaker changes, limited to reduced monocytes and increased B cells after one year (Supplementary Table S12D). The weakest and most delayed responses were observed in difficult TB cases, drug-resistant TB cases, and outbreak TB strain subgroups (Fig. 5E; Supplementary Figure S14; Supplementary Tables S12F–12H). At the individual level, patient trajectories revealed notable heterogeneity in both the *Thompson_SA* (Supplementary Figure S15) and *Tabone_Leicester*

(Supplementary Figure S16) cohorts. While population-level trends showed consistent reversal of TB-associated changes, patient-specific factors clearly influenced the magnitude and timing of recovery.

Overall, these findings highlight the temporal dynamics of immune recovery during ATT. The consistent pattern of declining monocytes and neutrophils alongside rising NK cells, CD4⁺ T cells, CD8⁺ T cells, and B cells reflects a reversal of TB-induced compositional shifts and is strongly associated with treatment efficacy (Fig. 5D and E). However, inter-patient variability underscores the need to account for individual and cohort-specific factors when interpreting immune responses to therapy.

Effect of confounding factors on blood cellular changes during TB development

Understanding how TB progression alters peripheral blood cell composition is crucial for identifying biomarkers and disease stages. However, these changes can be influenced by extrinsic factors. To address this, we conducted multi-cohort meta-comparisons across subgroups defined by local TB burden, age and HIV coinfection status (Fig. 1E; Supplementary Notes, Sect. 4).

First, we examined whether the local TB burden influenced the compositional changes in blood cells in different stages of TB (Supplementary Table S3). Comparisons between high- and low-burden settings revealed broadly consistent cellular patterns across disease stages, but with notable subgroup-specific differences (Fig. 6A; Supplementary Figure S17A; Supplementary Table S13). In LTBI individuals, both subgroups showed overall trends similar to the global analysis (Fig. 2A), yet neutrophils did not change significantly in either subgroup, and NK cell reductions were observed only in low-burden cohorts. Among ATB patients, cellular changes in both subgroups also mirrored global patterns (Fig. 3A). However, in asymptomatic LTBI NP individuals, monocytes increased significantly only in the low-burden cohorts (Fig. 6A; Supplementary Figure S17A). More broadly, monocytes, neutrophils, NK cells, and B cells differed significantly between high- and low-burden LTBI groups; monocytes, CD4⁺ T cells, CD8⁺ T cells, and B cells differed in ATB patients; and monocytes, CD4⁺ T cells, NK cells, and B cells differed in LTBI NP individuals. Overall, individuals in low-burden regions exhibited more pronounced changes across stages, likely reflecting the immunological naivete of UI individuals in these settings. Second, we explored the effects of age on blood cellular changes during TB progression by grouping individuals into age categories: adolescents, adults, and seniors (Supplementary Tables S3, S6). For LTBI individuals, the compositional changes in adults (Fig. 6B) were largely consistent with those observed in the global cohort analysis (Fig. 2A; Supplementary Figure S17B; Supplementary Table S14). However, there was a significant increase in B cells exclusively in the adult subgroup. In contrast, adolescents and seniors presented less pronounced changes

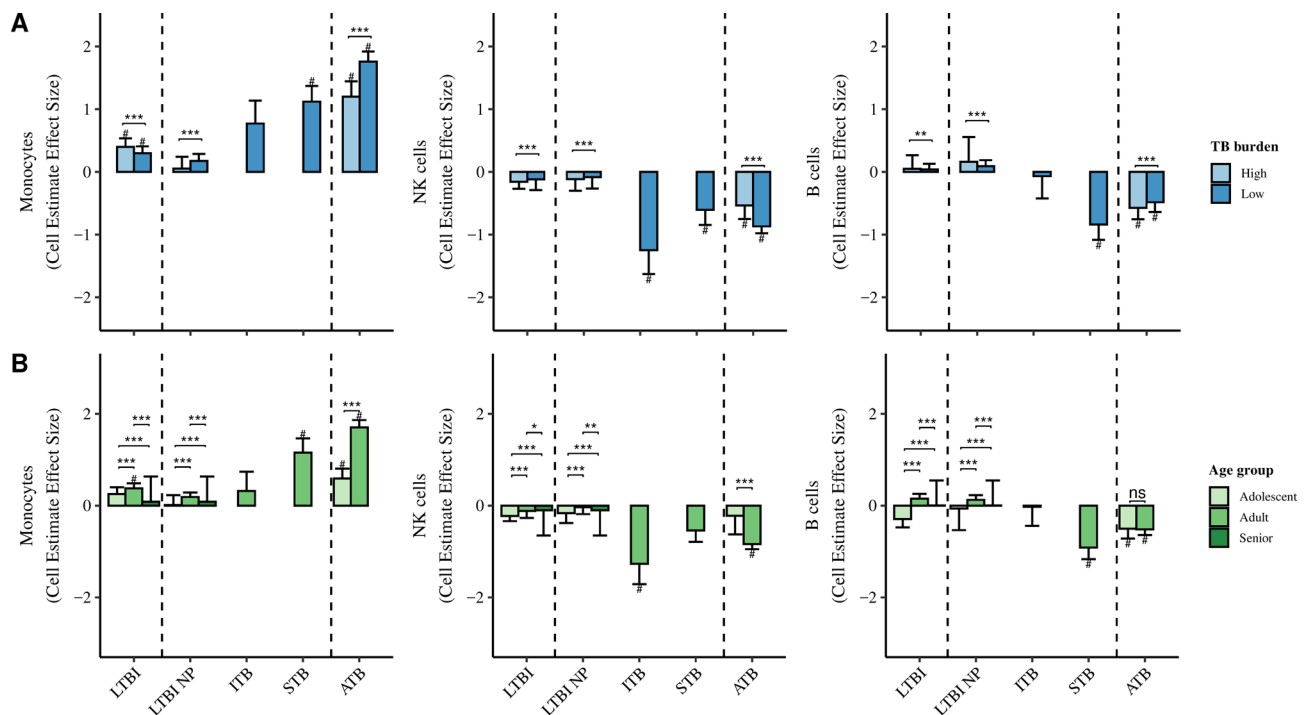


Fig. 6. Impact of confounding factors on blood cellular changes during TB development. **(A)** Bar plots displaying the compositional changes in monocytes, NK cells, and B cells between TB high- and low-burden countries. # indicates a significant compositional change in multi-cohort meta-analysis with an *FDR* < 0.1. The error bars represent the 95% confidence intervals of the effect size (*ES*) values. The statistical significance of compositional differences between two subgroups was assessed via two-tailed unpaired *t* tests with *Benjamini-Hochberg* correction. The significance thresholds are denoted as follows: ns (not significant); *P*-value > 0.1; *: *P*-value < 0.1; **: *P*-value < 0.01; and ***: *P*-value < 0.001. **(B)** Bar plots illustrating the compositional changes in monocytes, neutrophils, and NK cells across different age groups, including adolescents, adults and seniors. The *x*-axis represents TB disease stages, and the *y*-axis denotes cohort-summary *ES*s.

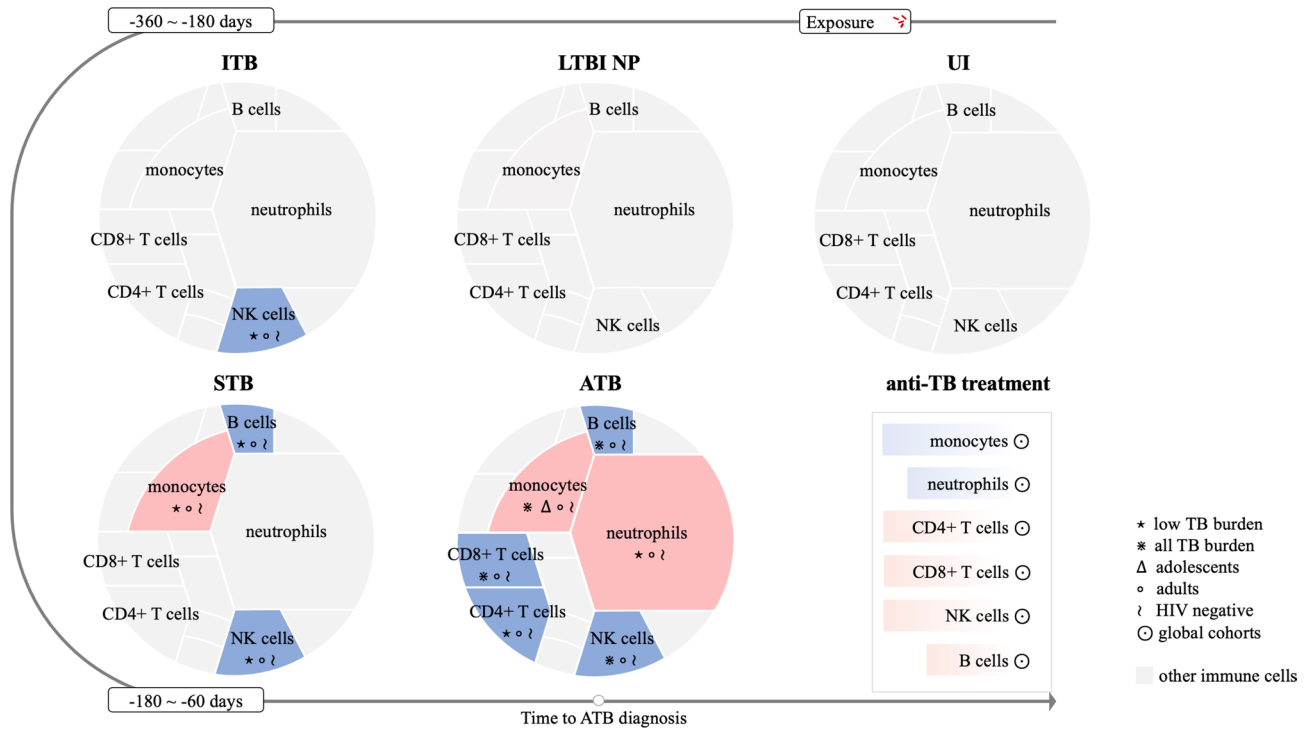


Fig. 7. The trajectories of peripheral blood cellular changes throughout TB development and treatment.

in blood cell composition, with no significant changes in most cell types, although adolescents presented a notable decrease in B-cell proportions at the LTBI stage (Fig. 6B; Supplementary Figure S17B). These age-related differences persisted across other disease stages, including ATB patients and individuals in asymptomatic disease states. These results suggest that adults experience more significant and consistent blood cellular changes than adolescents or seniors do. This may be explained by the generally immunocompromised status of adolescents (due to ongoing immune system development) and seniors (due to the aging immune system). Third, we also evaluated the impact of HIV coinfection. Because of limited sample sizes (Supplementary Tables S3, S6), results were largely indistinguishable from analyses of HIV-negative individuals, with overall compositional changes closely matching those in the global cohorts (Supplementary Figure S17; Supplementary Table S15).

Together, these analyses indicate that local TB burden and age significantly influence TB-associated shifts in peripheral blood cell composition, whereas HIV coinfection could not be fully assessed due to limited data. In general, individuals from low-burden regions and adults displayed the most pronounced cellular changes, while adolescents and seniors exhibited weaker responses. These findings highlight the need to account for demographic and epidemiological context when interpreting blood-based biomarkers of TB progression.

Discussion

In this study, we performed a comprehensive analysis of cellular compositional changes in the peripheral blood of individuals with diverse TB-related clinical phenotypes. Building upon a prior multi-cohort study of immune correlates of *Mtb* infection¹⁷, we reanalyzed 5,902 peripheral blood samples from 43 publicly available transcriptomic datasets. A key advance of our work was the reclassification of these samples using a recently proposed framework that captures the full spectrum of TB disease³⁸. This approach allowed us to subdivide asymptomatic LTBI individuals into three biologically distinct states - LTBI NP, ITB, and STB, thus refining the characterization of early disease heterogeneity²¹. Our analysis also incorporated post-treatment samples, enabling us to examine immune dynamics before and after ATT. By incorporating the largest number of cohorts and samples and systematically accounting for potential confounders such as local TB burden, age, and HIV coinfection, we provide, to our knowledge, the most extensive multi-cohort investigation of cellular dynamics in TB to date.

We found that trajectories of peripheral immune cell changes emerge early, beginning during LTBI stage. The earliest signal was an increase in proportion of monocytes, followed by broader alterations as individuals progressed toward active disease (Figs. 2 and 7). The transition to ATB was marked by widespread lymphopenia and expansion of myeloid lineages, changes that were reversible following successful ATT (Figs. 5 and 7). These findings are consistent with prior reports^{5,8,11,13-17,39-41} and reinforce the dynamic nature of immune remodeling across the TB spectrum. Specifically, circulating monocytes, particularly CD16⁺ subsets, expanded with disease progression and correlated with severity⁴². These nonclassical monocytes play key roles in antigen presentation, T-cell stimulation, and macrophage differentiation. Neutrophils also demonstrated a dual role: protective during early infection but pathogenic during established ATB⁴³, where elevated proportions were associated with poor clinical outcomes and delayed culture conversion^{44,45}. Conversely, lymphocyte subsets,

including IFN- γ -producing CD4⁺ and CD8⁺ T cells⁴⁶, B cells⁴⁷, and NK cells⁴⁸, declined with advancing disease, underscoring their importance in protective immunity^{46–48}. Our multi-cohort design also revealed nuanced findings not consistently reported in smaller studies. For example, while Roy Chowdhury et al. described NK cell expansion in LTBI¹⁷, we observed a trend toward decreased NK proportions in this group, though not statistically significant (Fig. 2A). This discrepancy likely reflects heterogeneity in the proportion of incipient and subclinical cases within LTBI cohorts¹⁷, as well as inter-cohort variability. Indeed, while seven of fourteen individual cohorts showed increased or near-increased NK proportions, the aggregate analysis indicated an overall decline (Fig. 2B). Such results highlight the value, and the challenge, of integrating diverse datasets, where cohort heterogeneity both enriches generalizability and complicates interpretation.

A central contribution of our work is the delineation of immune changes at asymptomatic stages of TB progression. We observed no significant compositional shifts in cell proportions in limited LTBI NP cohorts (Figs. 3 and 7). As the disease progresses to the incipient stage, a reduction in NK cells is observed, followed by a decrease in B cells during the subclinical stage. These cellular alterations are pivotal, as they mark the transition from latent infection to active disease. The earliest cellular change in TB progression is the reduction in NK cells during the ITB stage, which persists until TB diagnosis. Circulating NK cells exhibit enhanced cytotoxic activity and interact with peripheral B and T cells under inflammatory conditions to control *Mtb* infection¹⁷. The gradual depletion of NK cells, particularly CD3⁻ CD7⁺ GZMB⁺ NK cells, is strongly associated with TB progression. This pattern has been observed in a *Chinese* cohort¹⁴ as well as in global cohorts spanning three continents¹⁷, further highlighting the significance of NK cell dynamics in TB progression. In contrast, changes in B lymphocytes occur relatively later, during the STB stage, and are marked by a significant decrease in blood B cells. This decrease has also been linked to human TB in previous studies^{12,35,49}. The timeline of these cellular changes is consistent with the general pattern of immune responses, as adaptive immune changes often occur later than innate immune responses. Moreover, this pattern of compositional changes in circulating immune cells is recapitulated in the temporal analysis of blood cell compositions in global longitudinal cohorts (Fig. 4). The earliest compositional change in TB progression is an increase in monocytes one and a half years before diagnosis. A decrease in B cells and an increase in neutrophils subsequently emerge between six and two months before diagnosis, followed by a decline in NK cells 21 days prior to TB diagnosis. Combined with the analysis of TB progression stages over time, timepoints more than 180 days before diagnosis approximate subclinical stages at the population level, while substantial inter-individual heterogeneity remains. Taken together, our findings provide a comprehensive view of the cellular changes that occur throughout TB development, offering valuable insights into the dynamic interplay between innate and adaptive immune responses and their roles in TB progression.

Despite these consistent trends, substantial heterogeneity was evident across cohorts and individuals (Figs. 2, 3, 4 and 5; Supplementary Figures S5, S7–S13, S15, S16). This variability has also been noted in previous studies, such as differences in B-cell compositional changes across cohorts¹⁷ and varying transcriptional activities of TB signatures among individuals²⁸. This heterogeneity may be attributed to the immune endotypes of TB patients, as TB is not a monomorphic disease⁵⁰. The host response to *Mtb* infection involves two distinct molecular pathways and pathologies. Endotype A is characterized by increased expression of genes related to inflammation and immunity, whereas endotype B is characterized by heightened activity in metabolism and proliferation pathways. These two mechanisms may influence cellular compositional changes during TB progression differently, adding complexity to the observed heterogeneity. However, the precise correlations between these endotypes and the variability in cellular changes remain unclear and warrant further investigation to better understand the underlying mechanism driving these differences.

Cellular changes in circulating blood cells serve as valuable indicators of the disease state and patient prognosis. For example, Bogan et al. identified KLRD-1-expressing NK cells as potential biomarkers for influenza susceptibility⁵¹. In human TB, the monocyte-to-lymphocyte ratio (MLR) has been recognized as an effective biomarker for diagnosing TB and monitoring the efficacy of anti-TB therapy⁸. However, the most pressing challenge in TB diagnosis is the early identification of TB progressors during the asymptomatic stage⁵². STB patients, despite having no clinical symptoms, contribute significantly to *Mtb* transmission²³. Differentiating ITB and STB patients from LTBI individuals and providing preventive treatment at early TB stages is the most effective strategy for TB prevention⁵³. Unfortunately, many early-stage TB patients lack radiologic abnormalities or microbiologic evidence, complicating their identification. The blood transcriptome has been extensively investigated for TB diagnosis, leading to the discovery of several transcriptional signatures for early-stage TB detection^{33–36,39,54–56}. For example, Zak et al. conducted a longitudinal study of healthy adolescents infected with *Mtb* in *South Africa*, prospectively collecting blood samples over two years and profiling their transcriptomes in this ACS cohort³³. They identified a 16-gene signature capable of predicting individuals at risk of developing ATB up to 12 months preceding TB. However, a promising validation study revealed that these blood prognostic signatures meet WHO benchmark requirements only when they are applied 3–6 months before TB diagnosis³¹. When tested in people living with HIV prior to antiretroviral therapy, their performance did not exceed that of a simple C-reactive protein (CRP) test and fell short of WHO targets⁵⁷. To improve their clinical utility, interferon-independent biomarkers need to be incorporated into these host-response signatures to increase their accuracy⁵⁷. Our findings revealed a specific decrease in NK cells during the transition from LTBI NP to ITB, a change that is common across multiple global cohorts and independent of transcriptional pathway activities. This compositional change shows strong potential as a cellular biomarker to distinguish ATB progressors from non-progressors at an early stage, offering a promising tool for improving TB diagnosis and prevention. Although cell type proportions hold promise for distinguishing stages of TB progression, the development and validation of a robust and specific classifier will require additional infection-related datasets and further in-depth investigation.

This study also has several limitations. First, we restricted analyses to six major blood cell types, precluding assessment of rarer populations implicated in TB, such as the CD3⁻ CD7⁺ GZMB⁺ NK subsets¹⁴ or NK-like

CD8⁺ $\gamma\delta$ T cells¹⁵. Integrating single-cell RNA-seq datasets in future work would enable higher-resolution deconvolution of blood mixtures²⁶. Second, the number of cohorts and samples used in multicohort comparisons of certain subgroups, such as STB and ITB patients, is relatively small. This limitation arises when TB-related samples are further divided by age or HIV coinfection status, reducing the statistical power of subgroup analyses. Third, our meta-analysis was not supported by experimental validation with flow cytometry or CyTOF due to limited availability of such datasets. Nonetheless, the biological plausibility of the findings, consistency with prior studies, and observed reversibility of changes post-ATT strengthen confidence in the results. Future studies addressing these limitations could provide a more comprehensive understanding of TB progression and its associated immune dynamics.

In conclusion, our multi-cohort study maps the temporal and stage-specific evolution of immune cell composition across the TB spectrum. By integrating thousands of samples spanning diverse global populations, we identify early depletion of NK cells and later B-cell loss as hallmarks of asymptomatic progression, and we situate these events within a broader framework of immune remodeling. These findings not only deepen our understanding of TB immunopathogenesis but also highlight NK cell dynamics as a promising avenue for early biomarker development and targeted prevention strategies.

Data availability

The original data of all public datasets are freely accessible in the *GEO* or *ArrayExpress* databases, while the processed data are available in supplementary tables.

Received: 7 April 2025; Accepted: 19 September 2025

Published online: 27 October 2025

References

- World Health Organization. *Global Tuberculosis Report 2024*. (2024).
- World Health Organization. *The End TB Strategy*. (2015). <https://www.who.int/publications/i/item/WHO-HTM-TB-2015-19>
- Uplekar, M. et al. WHO's new end TB strategy. *Lancet* **385**, 1799–1801. [https://doi.org/10.1016/s0140-6736\(15\)60570-0](https://doi.org/10.1016/s0140-6736(15)60570-0) (2015).
- Singhania, A., Wilkinson, R. J., Rodrigue, M., Haldar, P. & O'Garra, A. The value of transcriptomics in advancing knowledge of the immune response and diagnosis in tuberculosis. *Nat. Immunol.* **19**, 1159–1168. <https://doi.org/10.1038/s41590-018-0225-9> (2018).
- Ernst, J. D. The immunological life cycle of tuberculosis. *Nat. Rev. Immunol.* **12**, 581–591. <https://doi.org/10.1038/nri3259> (2012).
- Sia, J. K. & Rengarajan, J. Immunology of Mycobacterium tuberculosis infections. *Microbiol. Spectr.* **7**. <https://doi.org/10.1128/microbiolspec.GPP3-0022-2018> (2019).
- Mayer-Barber, K. D. & Sher, A. Cytokine and lipid mediator networks in tuberculosis. *Immunol. Rev.* **264**, 264–275. <https://doi.org/10.1111/imr.12249> (2015).
- Adane, T. et al. Accuracy of monocyte to lymphocyte ratio for tuberculosis diagnosis and its role in monitoring anti-tuberculosis treatment: systematic review and meta-analysis. *Med. (Baltim)*. **101**, e31539. <https://doi.org/10.1097/MD.00000000000031539> (2022).
- Kroidl, I. et al. Assessment of tuberculosis disease activity in people infected with Mycobacterium tuberculosis and living with HIV: A longitudinal cohort study. *Eclinicalmedicine* **49**, 101470. <https://doi.org/10.1016/j.eclinm.2022.101470> (2022).
- Chaussabel, D., Pascual, V. & Banchereau, J. Assessing the human immune system through blood transcriptomics. *BMC Biol.* **8**, 1–14. <https://doi.org/10.1186/1741-7007-8-84> (2010).
- Berry, M. P. R. et al. An interferon-inducible neutrophil-driven blood transcriptional signature in human tuberculosis. *Nature* **466**, 973–977. <https://doi.org/10.1038/nature09247> (2010).
- Moreira-Teixeira, L. et al. Mouse transcriptome reveals potential signatures of protection and pathogenesis in human tuberculosis. *Nat. Immunol.* **21**, 464–476. <https://doi.org/10.1038/s41590-020-0610-z> (2020).
- Nathan, A. et al. Multimodally profiling memory T cells from a tuberculosis cohort identifies cell state associations with demographics, environment and disease. *Nat. Immunol.* **22**, 781–793. <https://doi.org/10.1038/s41590-021-00933-1> (2021).
- Cai, Y. et al. Single-cell transcriptomics of blood reveals a natural killer cell subset depletion in tuberculosis. *EBioMedicine* **53**, 102686. <https://doi.org/10.1016/j.ebiom.2020.102686> (2020).
- Roy Chowdhury, R. et al. NK-like CD8(+) gammadelta T cells are expanded in persistent Mycobacterium tuberculosis infection. *Sci. Immunol.* **8**, eade3525. <https://doi.org/10.1126/sciimmunol.ade3525> (2023).
- Lyu, M. et al. Single-Cell sequencing reveals functional alterations in tuberculosis. *Adv. Sci. (Weinh)*. **11**, e2305592. <https://doi.org/10.1002/adv.202305592> (2024).
- Roy Chowdhury, R. et al. A multi-cohort study of the immune factors associated with M. tuberculosis infection outcomes. *Nature* **560**, 644–648. <https://doi.org/10.1038/s41586-018-0439-x> (2018).
- Kalesinskas, L., Gupta, S. & Khatri, P. Increasing reproducibility, robustness, and generalizability of biomarker selection from meta-analysis using bayesian methodology. *PLoS Comput. Biol.* **18**, e1010260. <https://doi.org/10.1371/journal.pcbi.1010260> (2022).
- Sweeney, T. E., Haynes, W. A., Vallania, F., Ioannidis, J. P. & Khatri, P. Methods to increase reproducibility in differential gene expression via meta-analysis. *Nucleic Acids Res.* **45**, e1. <https://doi.org/10.1093/nar/gkw797> (2017).
- Coussens, A. K. et al. Classification of early tuberculosis states to guide research for improved care and prevention: an international Delphi consensus exercise. *Lancet Respir Med.* **12**, 484–498. [https://doi.org/10.1016/S2213-2600\(24\)00028-6](https://doi.org/10.1016/S2213-2600(24)00028-6) (2024).
- Drain, P. K. et al. Incipient and subclinical tuberculosis: a clinical review of early stages and progression of infection. *Clin. Microbiol. Rev.* **31**, e00021–e00018. <https://doi.org/10.1128/cmr.00021-18> (2018).
- Stuck, L. et al. Prevalence of subclinical pulmonary tuberculosis in adults in community settings: an individual participant data meta-analysis. *Lancet Infect. Dis.* [https://doi.org/10.1016/s1473-3099\(24\)00011-2](https://doi.org/10.1016/s1473-3099(24)00011-2) (2024).
- Nguyen, H. V., Tiemersma, E., Nguyen, N. V., Nguyen, H. B. & Cobelens, F. Disease transmission by patients with subclinical tuberculosis. *Clin. Infect. Dis.* **76**, 2000–2006. <https://doi.org/10.1093/cid/ciad027> (2023).
- Clough, E. et al. NCBI GEO: archive for gene expression and epigenomics data sets: 23-year update. *Nucleic Acids Res.* **52**, D138–D144. <https://doi.org/10.1093/nar/gkad965> (2024).
- Sarkans, U. et al. From arrayexpress to biostudies. *Nucleic Acids Res.* **49**, D1502–D1506. <https://doi.org/10.1093/nar/gkaa1062> (2021).
- Newman, A. M. et al. Determining cell type abundance and expression from bulk tissues with digital cytometry. *Nat. Biotechnol.* **1–10**. <https://doi.org/10.1038/s41587-019-0114-2> (2019).
- Pai, M. et al. Tuberculosis. *Nat. Rev. Dis. Primers.* **2**, 16076. <https://doi.org/10.1038/nrdp.2016.76> (2016).
- Tabone, O. et al. Blood transcriptomics reveal the evolution and resolution of the immune response in tuberculosis. *J. Exp. Med.* **218**, e20210915. <https://doi.org/10.1084/jem.20210915> (2021).

29. Zaidi, S. M. A. et al. Beyond latent and active tuberculosis: a scoping review of conceptual frameworks. *Eclinicalmedicine* **66**, 102332. <https://doi.org/10.1016/j.eclinm.2023.102332> (2023).
30. Tateosian, N. L., Morelli, M. P., Pellegrini, J. M. & Garcia, V. E. Beyond the clinic: the activation of diverse cellular and humoral factors shapes the immunological status of patients with active tuberculosis. *Int. J. Mol. Sci.* **24** <https://doi.org/10.3390/ijms24055033> (2023).
31. Gupta, R. K. et al. Concise whole blood transcriptional signatures for incipient tuberculosis: a systematic review and patient-level pooled meta-analysis. *Lancet Respir Med.* **8**, 395–406. [https://doi.org/10.1016/s2213-2600\(19\)30282-6](https://doi.org/10.1016/s2213-2600(19)30282-6) (2020).
32. Haynes, W. A. et al. Empowering Multi-Cohort gene expression analysis to increase reproducibility. *Pac. Symp. Biocomput.* **22**, 144–153. https://doi.org/10.1142/9789813207813_0015 (2017).
33. Zak, D. E. et al. A blood RNA signature for tuberculosis disease risk: a prospective cohort study. *Lancet* **387**, 2312–2322. [https://doi.org/10.1016/s0140-6736\(15\)01316-1](https://doi.org/10.1016/s0140-6736(15)01316-1) (2016).
34. Suliman, S. et al. Four-Gene Pan-African blood signature predicts progression to tuberculosis. *Am. J. Respir Crit. Care Med.* **197**, 1198–1208. <https://doi.org/10.1164/rccm.201711-2340oc> (2018).
35. Singhania, A. et al. A modular transcriptional signature identifies phenotypic heterogeneity of human tuberculosis infection. *Nat. Commun.* **9**, 2308. <https://doi.org/10.1038/s41467-018-04579-w> (2018).
36. Roe, J. et al. Blood transcriptomic stratification of short-term risk in contacts of tuberculosis. *Clin. Infect. Dis.* **70**, e2525. <https://doi.org/10.1093/cid/ciz252> (2019).
37. Thompson, E. G. et al. Host blood RNA signatures predict the outcome of tuberculosis treatment. *Tuberculosis* **107**, 48–58. <https://doi.org/10.1016/j.tube.2017.08.004> (2017).
38. Coussens, A. K. et al. Classification of early tuberculosis states to guide research for improved care and prevention: an international Delphi consensus exercise. *Lancet Respir Med.* [https://doi.org/10.1016/s2213-2600\(24\)00028-6](https://doi.org/10.1016/s2213-2600(24)00028-6) (2024).
39. Bloom, B. R. A half-century of research on tuberculosis: successes and challenges. *J. Exp. Med.* **220**, e20230859. <https://doi.org/10.1084/jem.20230859> (2023).
40. Kotov, D. I. et al. Early cellular mechanisms of type I interferon-driven susceptibility to tuberculosis. *Cell* **186**, 5536–5553 e5522 (2023). <https://doi.org/10.1016/j.cell.2023.11.002>
41. Scriba, T. J. et al. Sequential inflammatory processes define human progression from M. tuberculosis infection to tuberculosis disease. *PLoS Pathog.* **13**, e1006687. <https://doi.org/10.1371/journal.ppat.1006687> (2017).
42. Sampath, P., Moideen, K., Ranganathan, U. D. & Bethunaickan, R. Monocyte subsets: phenotypes and function in tuberculosis infection. *Front. Immunol.* **9**, 1726. <https://doi.org/10.3389/fimmu.2018.01726> (2018).
43. Lowe, D. M., Redford, P. S., Wilkinson, R. J., O'Garra, A. & Martineau, A. R. Neutrophils in tuberculosis: friend or foe? *Trends Immunol.* **33**, 14–25. <https://doi.org/10.1016/j.it.2011.10.003> (2012).
44. Carvalho, A. C. C. et al. Pre-Treatment neutrophil count as a predictor of antituberculosis therapy outcomes: A multicenter prospective cohort study. *Front. Immunol.* **12**, 661934. <https://doi.org/10.3389/fimmu.2021.661934> (2021).
45. Ndlovu, L. N. et al. Increased neutrophil count and decreased neutrophil CD15 expression correlate with TB disease severity and treatment response irrespective of HIV Co-infection. *Front. Immunol.* **11**, 1872. <https://doi.org/10.3389/fimmu.2020.01872> (2020).
46. Musvosvi, M. et al. T-cell biomarkers for diagnosis of tuberculosis: Candidate evaluation by a simple whole blood assay for clinical translation. *Eur. Respir J.* **51**. <https://doi.org/10.1183/13993003.00153-2018> (2018).
47. Joosten, S. A. et al. Patients with tuberculosis have a dysfunctional circulating B-Cell Compartment, which normalizes following successful treatment. *PLoS Pathog.* **12**, e1005687. <https://doi.org/10.1371/journal.ppat.1005687> (2016).
48. Abebe, F. Immunological basis of early clearance of Mycobacterium tuberculosis infection: the role of natural killer cells. *Clin. Exp. Immunol.* **204**, 32–40. <https://doi.org/10.1111/cei.13565> (2021).
49. Krause, R. et al. B cell heterogeneity in human tuberculosis highlights compartment-specific phenotype and functional roles. *Commun. Biol.* **7**, 584. <https://doi.org/10.1038/s42003-024-06282-7> (2024).
50. DiNardo, A. R. et al. Gene expression signatures identify biologically and clinically distinct tuberculosis endotypes. *Eur. Respir J.* **60**, 2102263. <https://doi.org/10.1183/13993003.02263-2021> (2022).
51. Bongen, E., Vallania, F., Utz, P. J. & Khatri, P. KLRD1-expressing natural killer cells predict influenza susceptibility. *Genome Med.* **10**, 45. <https://doi.org/10.1186/s13073-018-0554-1> (2018).
52. World Health Organization. *Consensus Meeting Report - Development of a Target Product Profile (TPP) and a Framework for Evaluation for a Test for Predicting Progression from Tuberculosis Infection to Active Disease.* (2017). <https://www.who.int/publications/i/item/WHO-HTM-TB-2017.18>
53. Horton, K. C., Richards, A. S., Emery, J. C., Esmail, H. & Houben, R. M. G. J. Reevaluating progression and pathways following Mycobacterium tuberculosis infection within the spectrum of tuberculosis. *Proc. Natl. Acad. Sci.* **120**, e2221186120. <https://doi.org/10.1073/pnas.2221186120> (2023).
54. Leong, S. et al. Cross-validation of existing signatures and derivation of a novel 29-gene transcriptomic signature predictive of progression to TB in a Brazilian cohort of household contacts of pulmonary TB. *Tuberculosis* **120**, 101898. <https://doi.org/10.1016/j.tube.2020.101898> (2020).
55. Sivakumaran, D. et al. Host blood-based biosignatures for subclinical TB and incipient TB: A prospective study of adult TB household contacts in Southern India. *Front. Immunol.* **13**, 1051963. <https://doi.org/10.3389/fimmu.2022.1051963> (2023).
56. Esmail, H., Cobelens, F. & Goletti, D. Transcriptional biomarkers for predicting development of tuberculosis: progress and clinical considerations. *Eur. Respir J.* **55**, 1901957. <https://doi.org/10.1183/13993003.01957-2019> (2020).
57. Mann, T. et al. Blood RNA biomarkers for tuberculosis screening in people living with HIV before antiretroviral therapy initiation: a diagnostic accuracy study. *Lancet Glob Heal.* [https://doi.org/10.1016/s2214-109x\(24\)00029-9](https://doi.org/10.1016/s2214-109x(24)00029-9) (2024).

Author contributions

W.G., M.W., and X.X. conceived the study. S.Z., H.Y., Q.D., K.W., Y.M., and Y.N. contributed to the data analysis. W.G., M.W., X.X., and C.C. interpreted the results, and S.Z. and W.G. wrote the manuscript. All the authors read, revised and approved the final version of the manuscript.

Funding

This work was supported by the National Key R&D Program of China (Nos. 2022YFC3500200, 2022YFC3500202, 2023YFC2307300), the National Natural Science Foundation of China (Nos. 81930117, 82430122), the Jiangsu Provincial Social Development and Clinical Frontier Technology Project (BE2023790), and the Respiratory Infectious Diseases Clinical Medical Center of Suzhou (No. Szlcyxz202108).

Declarations

Competing interests

The authors declare no competing interests.

Additional information

Supplementary Information The online version contains supplementary material available at <https://doi.org/10.1038/s41598-025-21181-5>.

Correspondence and requests for materials should be addressed to S.Z. or W.G.

Reprints and permissions information is available at www.nature.com/reprints.

Publisher's note Springer Nature remains neutral with regard to jurisdictional claims in published maps and institutional affiliations.

Open Access This article is licensed under a Creative Commons Attribution-NonCommercial-NoDerivatives 4.0 International License, which permits any non-commercial use, sharing, distribution and reproduction in any medium or format, as long as you give appropriate credit to the original author(s) and the source, provide a link to the Creative Commons licence, and indicate if you modified the licensed material. You do not have permission under this licence to share adapted material derived from this article or parts of it. The images or other third party material in this article are included in the article's Creative Commons licence, unless indicated otherwise in a credit line to the material. If material is not included in the article's Creative Commons licence and your intended use is not permitted by statutory regulation or exceeds the permitted use, you will need to obtain permission directly from the copyright holder. To view a copy of this licence, visit <http://creativecommons.org/licenses/by-nc-nd/4.0/>.

© The Author(s) 2025